Two Dominant Mutations in the Mouse *Fused* Gene Are the Result of Transposon Insertions

Thomas J. Vasicek,*,[1] Li Zeng,[†] X-J. Guan,* Tong Zhang,[†] Frank Costantini[†] and Shirley M. Tilghman*

**Howard Hughes Medical Institute and Department of Molecular Biology, Princeton University, Princeton, New Jersey 08544 and* [†]*Department of Genetics, Columbia College of Physicians and Surgeons, New York, New York 10032*

Manuscript received April 29, 1997
Accepted for publication June 30, 1997

ABSTRACT

The mouse *Fused* locus encodes a protein that has been implicated in the regulation of embryonic axis formation. The protein, which has been named Axin to distinguish it from the product of the unrelated *Drosophila melanogaster* gene *fused*, contains regions of similarity to the RGS (regulators of G-protein signaling) family of proteins as well as to dishevelled, a protein that acts downstream of Wingless in *D. melanogaster*. Loss-of-function mutations at *Fused* lead to lethality between days 8 and 10 of gestation. Three dominant mutations result in a kinked tail in heterozygotes. Two of the dominant mutations, *Fused* and *Knobbly*, result from insertions of intracisternal A particle retrotransposons into the gene. The insertion in *Fused*, within the sixth intron, creates a gene that produces wild-type transcripts as well as mutant transcripts that initiate at both the authentic promoter and the 3′-most long terminal repeat of the insertion. *Knobbly*, an insertion of the retrotransposon into exon 7, precludes the production of wild-type protein. Thus the *Fused* homozygote is viable whereas *Knobbly* is a recessive embryonic lethal. In both mutants the dominant kink-tailed phenotype is likely to result from the synthesis of similar amino-terminal fragments of Axin protein that would contain the RGS domain, but lack the dishevelled domain.

THE mouse *Fused* locus (*Fu*) was identified 60 years ago as the result of a dominant mutation whose phenotype is a kinky tail (REED 1937). Although homozygotes of the original allele, Fu^{Fused} (Fu^{Fu}), are viable, they sometimes display deafness and other neurological and urogenital defects, in addition to the kinked tail (REED 1937; DUNN and GLUECKSOHN-WAELSCH 1954; THEILER and GLUECKSOHN-WAELSCH 1956; DEOL 1966). Two additional alleles of *Fu* were subsequently identified, Fu^{Kinky} (Fu^{Ki}) and $Fu^{Knobbly}$ (Fu^{Kb}) (CASPARI and DAVID 1940; JACOBS-COHEN *et al.* 1984). While sharing the kinked tail phenotype of Fu^{Fu} as heterozygotes, Fu^{Ki} and Fu^{Kb} homozygotes die in utero, between 8 and 10 days post coitem (GLUECKSOHN-SCHOENHEIMER 1949; JACOBS-COHEN *et al.* 1984). The embryos display complete or partial duplication of axial structures, neural tube malformations and overgrowth of embryonic ectoderm, suggesting that the *Fu* gene may play a role in axis specification.

More recently a fourth allele of *Fu* was identified as a transgene insertion into the gene, based on its failure to complement the embryonic lethality of Fu^{Kb} (PERRY *et al.* 1995). Unlike the other alleles, Fu^{Tg1} is fully recessive and displays no tail kinks. However Fu^{Tg1} homozygous embryos are indistinguishable from Fu^{Kb} homozygotes or Fu^{Tg1}/Fu^{Kb} compound heterozygotes. These observations suggest that the dominant kinked tail phenotype is caused by a gain-of-function mutation at *Fu*, whereas the embryonic lethality is due to a loss-of-function of the gene. This conclusion is consistent with an earlier observation that a chromosome deletion that removes *Fu* has no heterozygous phenotype and fails to complement the embryonic lethality of Fu^{Ki} and Fu^{Kb} (GREENSPAN and O'BRIEN 1986). Furthermore $Fu^{Ki}/+/+$ trisomic mice have kinked tails, despite the presence of two wild-type copies of the gene (RUVINSKY and AGULNIK 1991). Thus it seems most likely that the three dominant alleles express the normal gene product inappropriately or express a mutant form of the protein.

Aided by the molecular access provided by the transgene insertion, the *Fu* gene was cloned and was shown to be broadly expressed during embryogenesis and adulthood (ZENG *et al.* 1997). The gene encodes several mRNAs, the longest of which contains the potential coding capacity for a 992-amino acid protein. To avoid confusion with the unrelated *Drosophila melanogaster* gene *fused*, we have renamed the mammalian *Fu* gene *Axin*, for axis inhibition.

The most striking aspect of the predicted amino acid sequence of Axin is a 130-amino acid-long domain in the amino terminal half of the protein that shares similarity to proteins known or predicted to be negative regulators of G-protein signaling. Thus the domain is referred to as the RGS domain, for regulators of G-protein signaling (KOELLE and HORVITZ 1996; DOHL-

Corresponding author: Shirley M. Tilghman, Department of Molecular Biology, Princeton University, Princeton, NJ 08544.
E-mail: stilghman@molbiol.princeton.edu

[1]*Present address:* Millennium Pharmaceuticals, Cambridge, MA 02139.

MAN and THORNER 1997). Proteins containing the RGS domain have been identified in eukaryotes from yeast to humans, though the sequence similarity among them rarely extends beyond the RGS domain itself. Two well characterized RGS-encoding genes are *egl-10* in *Caenorhabditis elegans* (KOELLE and HORVITZ 1996) and *SST2* in *S. cerevisiae* (CHAN and OTTE 1982; DIETZEL and KURJAN 1987; DOHLMAN *et al.* 1995). The *egl-10* mutation affects the timing of periodic behaviors such as egg laying and writhing and genetic analysis suggests that it does so by modulating the activity of $G_o\alpha$-1. The yeast recessive mutation *sst2* results in supersensitivity to mating pheromone via overstimulation of pheromone signaling through its G-protein-coupled seven-transmembrane-domain receptor.

By analogy to *egl-10* and *sst-2*, the axis duplications characteristic of loss-of-function mutations at *Axin* might be explained if the function of the protein is to suppress the formation of the primitive streak throughout the circumference of the egg cylinder except at the position that is destined to become the primitive streak. This model has been experimentally tested by injecting wild-type mouse *Axin* mRNA into the dorsal side of *Xenopus laevis* embryos, where it inhibited axis formation by interfering with signaling through the Wnt pathway (ZENG *et al.* 1997). A potential role for *Axin* in signaling in the Wnt pathway during gastrulation is also suggested by a region in its carboxy terminus that displays significant homology to the intracellular protein, dishevelled. *dishevelled* was originally identified in *D. melanogaster* as a gene that acts positively downstream in the *wingless* signaling pathway (KLINGENSMITH *et al.* 1994; NOORDERMEER *et al.* 1994; THEISEN *et al.* 1994).

In this article, the molecular nature of the mutations in two *Axin* dominant alleles, $Axin^{Fu}$ and $Axin^{Kb}$, is described. Both mutations result from the insertion of an intracisternal A particle (IAP) transposon into the *Axin* gene, resulting in very similar mRNA fusions between IAP RNA and *Axin* sequences. The precise locations of the two insertions explain the difference between the viabilities of $Axin^{Fu}$ and $Axin^{Kb}$ homozygotes and imply that both alleles result in the production of very similar amino terminal fragments of Axin that contain the RGS domain, but lack the dishevelled homology.

MATERIALS AND METHODS

Mice: BTBR Fu^{Kb}/+ animals, originally reported as BTBR Fu^{Ki}/+ (ROSSI *et al.* 1994), were obtained from Dr. WILLIAM DOVE at the University of Wisconsin. C3H Fu^{Kb}/+ animals were obtained from Dr. KAREN ARTZT at the University of Texas at Austin. 129/Rr Fu^{Fu}/Fu^{Fu} mice were obtained from the JACKSON Laboratory.

DNA analysis: For large preparations of DNA, tissues were homogenized for 45 sec with a polytron (Kinematica, Luzern, Switzerland) in 100 mM NaCl, 10 mM Tris.HCl pH 8.0, 50 mM EDTA at a concentration of 1.2 ml/g of tissue. The suspension was adjusted to 0.5% SDS and 0.2 mg/ml proteinase K and incubated at 55° for 4 hr. The solution was extracted with an equal volume of phenol, precipitated with 2 vol ethanol, and dissolved in H_2O. One-centimeter tail fragments were treated identically, except that the homogenization step was omitted and replaced with occasional vortexing during the incubation.

The DNAs were digested with restriction endonucleases according to the conditions provided by New England Biolabs and analyzed on 1.0% native agarose gels. The DNAs were transferred to Hybond-N+ membranes (CHOMCZYNSKI and SACCHI 1987) and crosslinked to the membranes with ultraviolet light (Stratalinker, Stratagene, La Jolla, CA). The filters were hybridized to the following probes generated by RT-PCR: an exon 2 probe that spans bases 363–812 in *Axin* cDNA, using the numbering system in ZENG *et al.* (1997) (primers 5′CATTGTTCACTGATGCAGAGTCCC3′ and 5′TGCCAG CTTCAGCCTCTTTTCC3′), an exon 6 probe containing bases 1631–2164 (primers 5′GCGTGTACGCATGGAGGA AG3′ and 5′CCACCAAAGGGCAAATCCCCAG3′) and an exon 10 probe containing bases 2904–3627 (primers 5′GAG GAAGTACGGGAGGATGAG3′ and 5′CATGTAAAGAGTCCG GTCCCG3′). The three probes were labeled by random-priming using DNA polymerase (FEINBERG and VOGELSTEIN 1984). The filters were washed under conditions of high stringency (0.1% SDS, 1.5 mM sodium citrate, 15 mM NaCl at 65°) and exposed to X-ray film.

DNA sequencing reactions were performed with Perkin-Elmer cycle sequencing TaqFS reagents and analyzed on a Perkin-Elmer-Applied Biosystems 373 automated sequencer.

Long segments of genomic DNA were amplified from 1.0-μg samples of mouse genomic DNA with the Perkin Elmer (Branchburg, NJ) XL PCR Kit in a 9600 thermal cycler. DNA primers flanking the IAP insertion sites were P1 in exon 6 (5′TTCCGAGAACGCAGGCACCAC3′) and P3 in exon 8 (5′CCCAGGACGCTCGATGGACAAG3′). The P2 primer within the IAP long terminal repeats (LTRs) was (5′CCATCT TGTGACGGCGAATGTG3′).

RNA analysis: RNA was prepared by LiCl/urea extraction (AUFFRAY and ROUGEON 1980) and analyzed on 0.8% agarose gels in the presence of 0.22 M formaldehyde with constant buffer recirculation (TSANG *et al.* 1992). The gels were blotted to Hybond-N+ nylon membranes (Amersham, UK) (CHOMCZYNSKI and SACCHI 1987). The filters were hybridized to the probes indicated above, along with an α-actin cDNA probe, to control for RNA loading.

cDNA cloning and RT-PCR: The Marathon cDNA Amplification kit (Clontech, Palo Alto, CA) was used to amplify the mutant cDNAs with 0.67 μl of a 60:1 mixture of Klentaq (Ab Peptides Inc., St. Louis, MO) in 50-μl reactions. Nested 5′ amplifications were done with the Marathon adaptor primer AP1 and the reverse primer beginning at base 2766 (5′CCCCACAGAAATAGTAGCCCACAAC3′) and then AP2 plus the reverse primer beginning at base 2720 (5′ACTCCCG CCACCTGCCTTTC3′). The resulting fragments were purified from agarose gels with QiaExII (Qiagen, Chatsworth, CA) and cloned into the TA cloning vector (Invitrogen, San Diego, CA). Further RT-PCR was performed with primers P1, P2 and P3 derived from the *Axin* cDNA and IAP sequences.

RNase protection: Uniformly labeled RNA probes were prepared according to the Ambion protocols using RNA polymerases and RNasin from Promega (Madison, WI) and [α-^{32}P]CTP (800 or 3000 Ci/mmol) from Dupont/NEN (Wilmington, DE). Hybridizations and RNase digestions were performed according to the Ambion (Austin, TX) RPA II™ kit except that after digestion the 200-μl reactions were treated with 0.15 μg/μl proteinase K and 0.5% SDS for 20 min at 37°, extracted with an equal volume of phenol/chloroform (3:1), and precipitated with ethanol. The reaction products were resolved on 5% acrylamide gels.

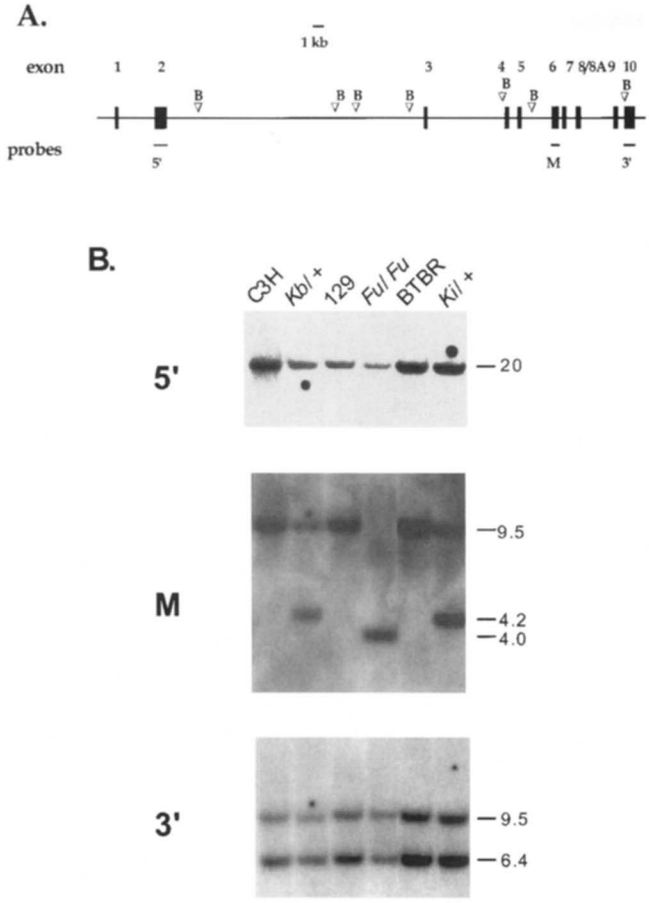

FIGURE 1.—Southern blot analysis of mutant alleles of *Axin*. (A) The exons of *Axin* are indicated by closed rectangles. Exon 2 encodes the RGS domain of the protein. Exon 8/8A is so designated because it has two alternative 3′ splice donor sites. The use of the 5′ proximal site yields an exon of 246 bp, while the 3′ site yields an exon containing an additional 108 bp. The positions of the relevant *Bam*HI sites for the analysis in B are drawn as inverted triangles and the hybridization probes are indicated at the bottom of the diagram. (B) Genomic DNA from the animals indicated was digested with *Bam*HI and analyzed by electrophoresis through an agarose gel. The DNAs were transferred to a membrane and hybridized to the radiolabeled probes indicated in A. The sizes of the genomic fragments in kb is indicated on the right.

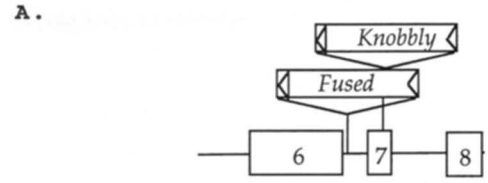

B. *Axin^{Fu}* insertion

```
exon 6-->        P1                                    |intron 6-->
TTCCGAGAACGCAGGCACCACCCTCAGTGCTGGGGATTTGGCCTTTGGgtgagtcttgat

                 |iap^Fu -->
ccagccttcttaatgttTCCAGTTGTTATTAGACGCGTTCTCACGACCGGCCAGGAAGAA

CACA..~5kb ...TACCCTTGGCTCATGCGCAGATTATTTGTTTACCAACTTAGAACAC

              P2                                  iap^Fu -->|
AGGATGTCAGCGCCATCTTGTGACGGCGAATGTGGGGGCGGCTTCCCACAtccagtgtgt

ccttgtatccaagtcatggttcatcgagtccgtggtcctgtggtgacttaatccagtcaa

agtcagacaatacccgggccaggggccagtcagactccaggccttgctatgactggatga

ggaggggcgcactttgggtttttcttgggctctggtcagcatggctctcctaccatagta

aaacagaccacagacagctgaccttcacagaggcctcagccttcacagtgggttgaagga

cttcttgttgagcttgagggttcaggaagtagcaagaaagaccagagtgacctcctatgt

 intron 6--> |exon 7-->
cttgttctcccagTGGTAAAACTAGTGCACCTTCCAAAAGAAACACCAAGAAGGCTGAAT
```

C. *Axin^{Kb}* insertion

```
exon 7                                  |iap^Kb-->
AGAACCAGAAGATCATGCAGTGGATCATTGAGGGAGAGAAGGTGTTATTAGACGCGTTCT
                                                      P2
CACGACCGGCCAGGAAGAACA.........~5.5 kb.......AGCGCCATCTTGTGAC
                          iap^Kb-->|exon 7
GGCGAATGTGGGGGCGGCTTCCCACAAGAAGGAGATCAGTAGACACCGGAAGGCAGGCCA

   |-->intron 7
TGGgtatgta
```

FIGURE 2.—DNA sequence of the IAP insertions into *Axin^{Fu}* and *Axin^{Kb}*. (A) The diagram indicates the positions of the IAP elements inserted into the *Axin* gene in the two mutant alleles. The boxes represent exons 6–8 of *Axin* and the triangles indicate the positions and orientations of the IAP LTRs. (B) The DNA sequence surrounding the *Axin^{Fu}* insertion, beginning at the 3′ end of exon 6. The positions of the intron 6 borders and the IAP insertion sites are indicated above the sequence. The primers, P1 and P2, used in Figure 5 are underlined, and the six-base duplications at the ends of the insertion sites are underlined and italicized. The intron sequence is in lowercase. (C) The DNA sequence surrounding the *Axin^{Kb}* insertion, beginning in exon 7. The border between exon 7 and intron 7 is indicated above the line, along with the IAP insertion site. Primer P2, used in Figure 5, is underlined and the six-base duplication at the site of IAP insertion is underlined and italicized.

RESULTS

Transposon insertions in the Axin gene: To screen for alterations in the structure of the *Axin* gene in the three *Axin* alleles, probes derived from exon 2 (5′), exon 6 (M) and exon 10 (3′) were hybridized to liver genomic DNA prepared from *Axin^{Fu}*/*Axin^{Fu}*, *Axin^{Ki}*/+ and *Axin^{Kb}*/+ animals (Figure 1). The patterns of bands observed with the 5′ and 3′ probes were identical in all mutant samples, and identical to 129/Rr, BTBR and C3H DNAs, the genetic backgrounds on which the mutations are maintained. However with the exon 6 probe, a novel band was evident in each mutant sample (Figure 1B).

Long-range PCR of genomic DNA with primers derived from exons 6 and 8 was utilized to characterize the nature of the change in genomic DNA. In all wild-type DNAs, a 1900-bp product was amplified, corresponding to parts of exons 6 and 8, all of exon 7 and two introns 352 and 1263 bp in length. In both *Axin^{Fu}*/*Axin^{Fu}* and *Axin^{Ki}*/+ DNAs, a novel ~7.5-kb band was amplified as well (data not shown). The band was cloned from each mutant sample and partially sequenced.

As shown in Figure 2B, the *Axin^{Fu}*-specific 7.5-kb band contained an insertion of an intracisternal A particle

(IAP) element, a member of the abundant family of murine transposable elements. The insertion began 35 bp downstream of exon 6, within intron 6. The IAP was of the [Δ] type (KUFF and LUEDERS 1988), having an internal 1.9-kb deletion relative to the full length IAP retrotransposon. However the 344-bp LTRs were intact and predicted by sequence comparison to known LTRs to contain bidirectional promoters (CHRISTY and HUANG 1988). The IAP genome was present in the opposite transcriptional orientation to the *Axin* gene and exhibited the typical 6-bp duplication of host genomic sequence at its ends.

The $Axin^{Ki}$-specific band also contained an [Δ] type IAP element, in this case inserted at 140 bp into exon 7 (Figure 2C). As was the case with $Axin^{Fu}$, the transcriptional orientation of the IAP was opposite to that of the wild-type *Axin* gene, and the LTRs were highly homologous to the consensus IAP sequence.

A surprising result was obtained when long-range PCR was performed on samples of DNA from our colony of $Axin^{Kb}$ mice, which we obtained in 1990 from Dr. KAREN ARTZT. The $Axin^{Kb}$ mutation was indistinguishable from that of $Axin^{Ki}$, a result that was confirmed by allele-specific PCR analysis with primers that uniquely amplified $Axin^{Ki}$ DNA (data not shown). The apparent identity of $Axin^{Ki}$ and $Axin^{Kb}$ was also consistent with the Southern blot data in Figure 1, where $Axin^{Ki}$ and $Axin^{Kb}$ exhibited the same novel band with the exon 6 probe. Fearing that we had inadvertently contaminated the $Axin^{Kb}$ stock with $Axin^{Ki}$ animals, we obtained $Axin^{Kb}$ DNA from Dr. MARY LYON at Harwell, who identified the original mutation. In these samples, the molecular character of the mutation was indistinguishable from $Axin^{Ki}$. Further discussions with Dr. WILLIAM DOVE, from whom we had obtained $Axin^{Ki}$, resolved the issue. His $Axin^{Ki}$ stock, obtained from Dr. JEAN-LOUIS GUENET, had actually been $Axin^{Kb}$. Thus the genetic mapping and the complementation studies that we previously reported (ROSSI *et al.* 1994; PERRY *et al.* 1995) had been performed with $Axin^{Kb}$, not $Axin^{Ki}$.

Transcription of $Axin^{Fu}$ and $Axin^{Kb}$: The impact of the IAP insertions at *Axin* on transcription was investigated by Northern blotting of RNAs isolated from adult tissues of $Axin^{Kb}/+$ and $Axin^{Fu}$ homozygous animals (Figure 3). With all probes, a 3.9-kb mRNA corresponding to the size of +/+ *Axin* RNA was detected in samples of brain, liver, kidney and spleen RNAs, reflecting the broad pattern of expression of the gene in adult (ZENG *et al.* 1997). The appearance of abundant wild-type transcript in $Axin^{Fu}$ homozygous RNA suggested that the intronic IAP element did not preclude correct RNA splicing between exons 6 and 7.

In addition to the wild-type transcript, the samples from the mutant animals also contained RNAs ranging in size from 1.7 to >12 kb. The sizes of these novel bands were very similar between the two mutant alleles, although the relative intensities of these bands differed among the tissue samples. With the 3′ exon 10 probe, an additional strongly hybridizing 1.7-kb RNA was detected in all $Axin^{Kb}/+$ tissues, most prominently in spleen RNA. A very faint band of slightly larger size was also observed in $Axin^{Fu}$ RNA, while no RNA in this size range was evident in +/+ RNA.

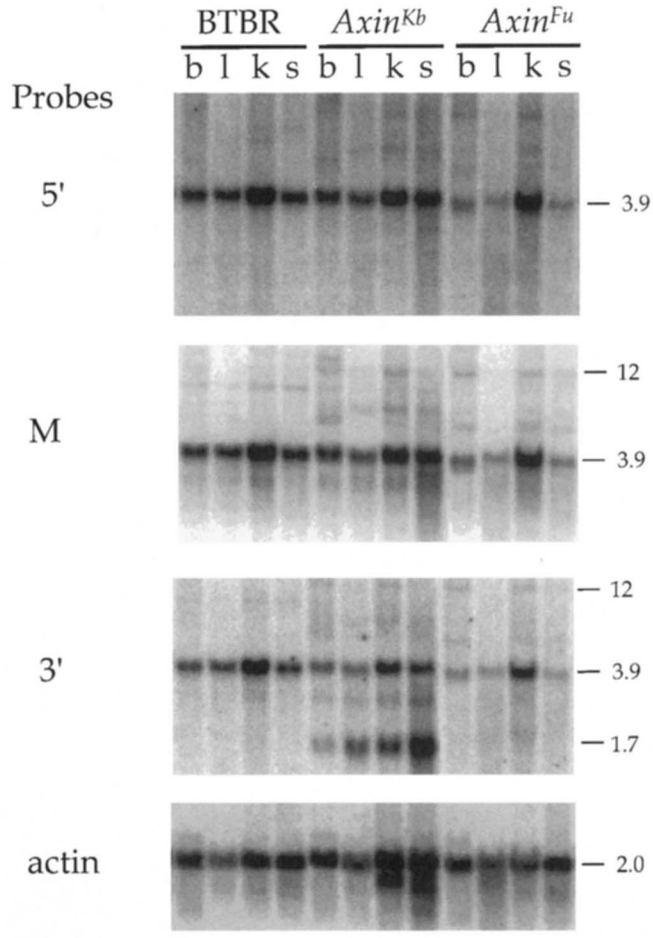

FIGURE 3.—Northern blot analysis of $Axin^{Fu}$ and $Axin^{Kb}$ RNAs. RNA was prepared from adult brain (b), liver (l), kidney (k) and spleen (s) from BTBR (+/+), $Axin^{Kb}/+$ and $Axin^{Fu}/Axin^{Fu}$ animals. The RNAs were separated by electrophoresis through an agarose gel, transferred to a membrane and hybridized successively to the radiolabeled probes described in Figure 1A, as well as an α-actin cDNA fragment to control for the amount of RNA in each lane. The sizes of the bands in kb are indicated on the right.

To characterize these novel RNAs in more detail, an RNase protection assay with a wild-type RNA probe generated from a cDNA clone that spanned the IAP insertion site in both alleles was utilized (Figure 4). The probe protected a full length 393-bp fragment in both +/+ and $Axin^{Fu}$ homozygous RNAs, confirming the conclusion that the $Axin^{Fu}$ IAP element did not prevent splicing of wild-type *Axin* transcripts. However, an additional band of 338 bp was also detected in $Axin^{Fu}$ samples. This size corresponds to the sum of the lengths of protected regions of exons 7 and 8, and implies that in addition to the normal splice, an aberrant splice to the

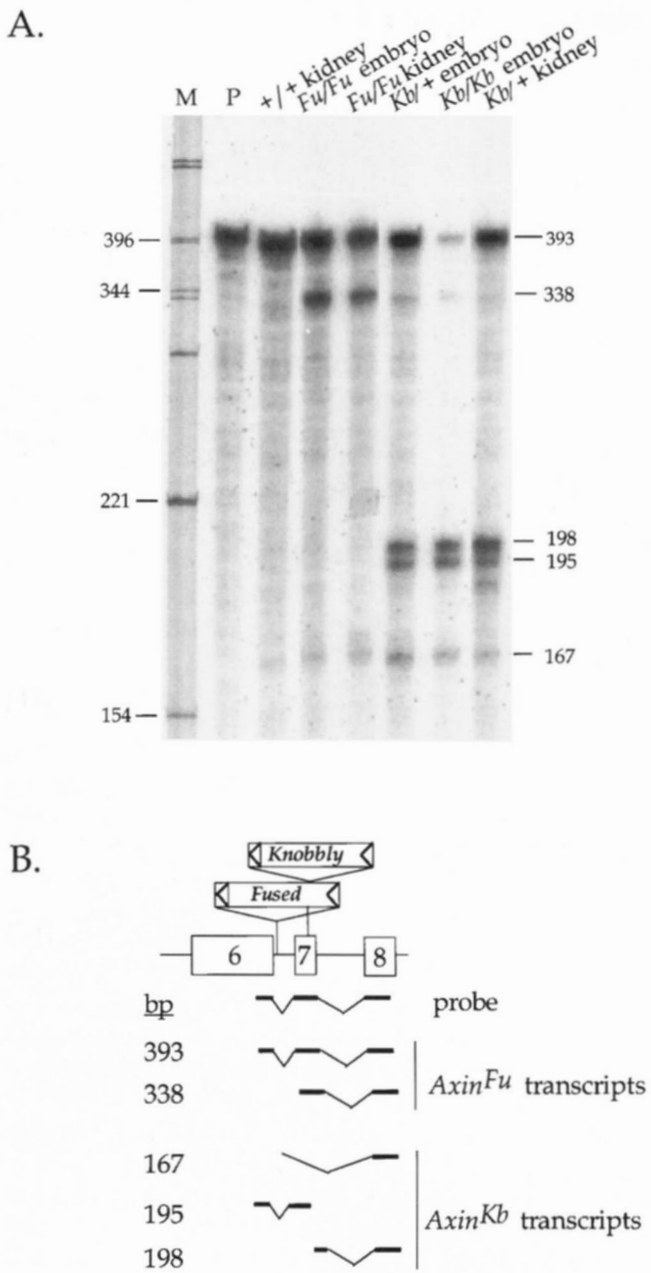

FIGURE 4.—RNase protection analysis of *Axin*^{Fu} and *Axin*^{Kb} RNAs. (A) The radiolabeled antisense probe indicated in B was hybridized to RNAs isolated from either adult kidney or e8.5 embryos from BTBR (+/+), *Axin*^{Fu}/*Axin*^{Fu} (*Fu/Fu*), *Axin*^{Kb}/+ (*Kb*/+) or *Axin*^{Kb}/*Axin*^{Kb} (*Kb/Kb*) animals as indicated. M, marker; P, undigested probe. The sizes of the marker fragments and the protected fragments in bp are indicated to the left and right of the figure, respectively. (B) The diagram indicates the positions of exons 6, 7 and 8 in the wild-type gene, and the positions of the IAP elements in the two mutant alleles. The probe was generated by RT-PCR on wild-type RNA using primers P1 and P3 (see Figures 2 and 5). The identities of the protected fragments in A are indicated.

5′ end of exon 7 was occurring from an upstream site, presumably within the IAP element itself.

The splicing variants generated by the *Axin*^{Kb} insertion were evident in both heterozygous tissues as well as homozygous embryo RNA. The prominent band at 195 bp corresponds to protection of the probe from RNA 5′ to the insertion site, while the 198-bp band reflects protection of RNA 3′ to the insertion site. The 167-bp band is contributed by protection of the exon 8 portion of the probe, which must be aberrantly spliced to an upstream site. The presence of a small amount of fully protected product in *Axin*^{Kb} homozygous embryonic RNA is likely due to maternal tissue contamination.

Generation of Axin-IAP fusion transcripts: The structure of *Axin*^{Kb} transcripts that initiated at the authentic *Axin* promoter was deduced from RNase protection assays as well as RT-PCR, followed by cDNA cloning and sequencing. Using primers in exons 6 and 8 in RT-PCR, four prominent products were obtained. The smallest band C in Figure 5, A and B, represents the splicing of exon 6 directly to exon 8. The next three bands (D–F) represent transcripts that splice from exon 6 to exon 7, and extend into the IAP to nucleotide 5596 in the consensus IAP sequence (MIETZ *et al.* 1987). They differ in their patterns of splicing within the IAP, with the smallest band resulting from splicing directly to exon 8, and the larger two are generated from either one or two additional splices within the IAP itself. These RNAs are predicted to be 5.0, 5.7 and 5.9 kb in size, consistent with the larger complex set of bands observed in the Northern analysis (Figure 3). The structure of these transcripts was confirmed by use of a primer, P2, that was present in both the 5′ and 3′ LTRs of the IAP element (data not shown).

The consensus IAP LTR contains a bidirectional promoter (CHRISTY and HUANG 1988), raising the possibility that transcripts could also initiate within the 3′-most LTR, with respect to the orientation of *Axin*. To investigate this possibility, an RNase assay was utilized. The probe contained the 3′ end of the IAP insertion, exons 7, 8, 8A and part of exon 9 (Figure 6A). The wild-type RNA protected 425- and 283-bp fragments, corresponding to the inclusion and exclusion of an alternatively spliced exon 8A, respectively. *Axin*^{Kb} RNA protected a full length 573-bp fragment and a faint 715-bp fragment, corresponding to transcripts that initiated at the authentic *Axin* promoter, and excluded or included the alternative exon, respectively. A 290-bp fragment identifies transcripts that initiated at the antisense promoter at the 3′ end of the LTR. The 3′-specific transcript presumably corresponds to the abundant 1.7-kb RNA that hybridized exclusively to the 3′ probe in the Northern analysis in *Axin*^{Kb}/+ RNA (Figure 3).

RT-PCR analysis of the *Axin*^{Fu} transcripts using exon 6 and 8 primers identified two major transcripts: the correctly spliced wild-type transcript (band A in Figure 5, A and C), as expected from RNase protection analysis (Figure 4), and an aberrant transcript in which the 3′ splice site of exon 6 was ignored and transcripts continued into intron 6 and the IAP itself to position 5596 (band B). The latter would generate an RNA 5.0 kb in

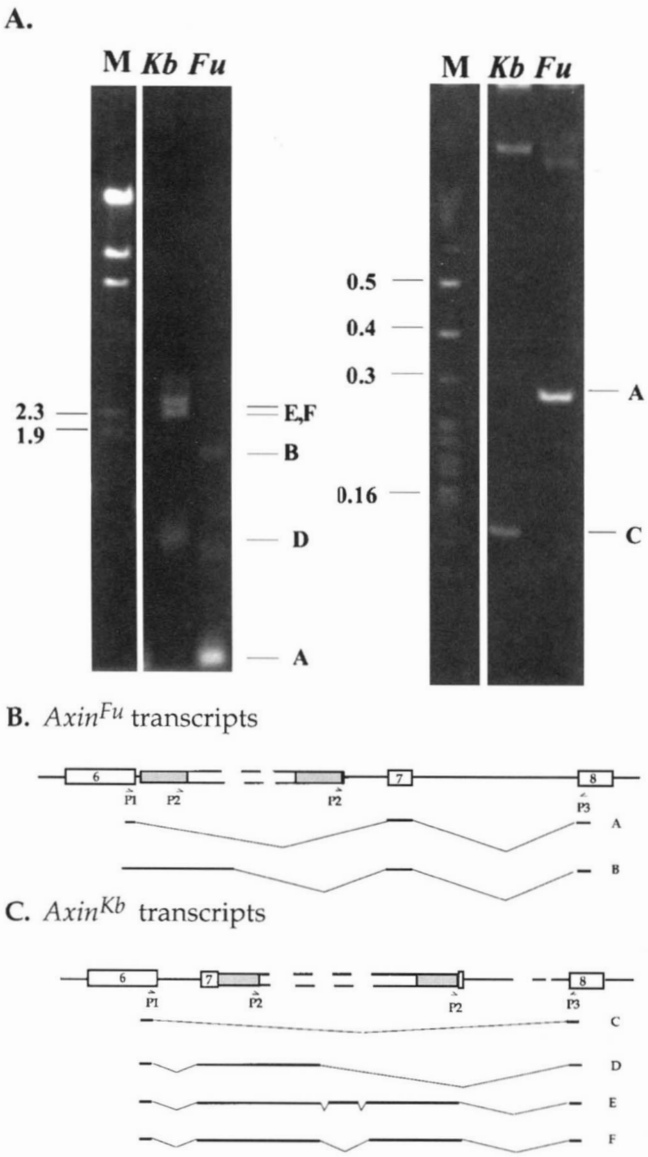

FIGURE 5.—RT-PCR Analysis of the mutant transcripts in $Axin^{Fu}$ and $Axin^{Kb}$. (A) RT-PCR on homozygous $Axin^{Fu}$ (*Fu*) and $Axin^{Kb}$ (*Kb*) embryonic RNA was performed using primers P1 within exon 6 and P3 in exon 8. The products were analyzed on an agarose gel (left) and an acrylamide gel (right) to resolve all products. The marker in the left panel is a *Hin*dIII digest of bacteriophage λ, while the marker on the right is a *Msp*I digest of pBR322. The sizes are indicated on the left of each figure. The letters on the right of each panel refer to the transcripts drawn in B and C. The structure of the transcripts identified by RT-PCR are drawn for $Axin^{Kb}$ (B) and $Axin^{Fu}$ (C). Exons 6–8 are indicated by open rectangles. The positions of the LTRs on the IAP insertions are indicated by shaded regions. The letters on the right refer to the bands in A. The *Fu*-specific band between A and B has not been characterized.

length. The use of primers P2 and P3 confirmed the structure of this transcript (data not shown).

To ask whether the $Axin^{Fu}$ allele also generated a transcript initiated from the 3′ LTR, an RNase protection probe was generated that spanned the 3′ end of the insertion site (Figure 6B). While the wild-type RNA protected a band of 283 bp, corresponding to exons 7 and 8, the $Axin^{Fu}$ RNA protected two additional bands, a fully protected probe suggesting transcription through the 3′ LTR and a smaller band consistent with initiation at the 3′ end of the LTR. The low intensity of the latter band is consistent with the low intensity of the ~1.8-kb 3′-specific band on Northern blots (Figure 3).

Thus both $Axin^{Kb}$ and $Axin^{Fu}$ generate fusion transcripts that initiate at the 5′ end of the *Axin* gene and proceed through the IAP element, as well as 3′ transcripts that initiate within the LTR of the IAP itself.

Putative protein products of $Axin^{Kb}$ and $Axin^{Fu}$: Conceptual translation of the $Axin^{Kb}$ transcripts predicts the synthesis of two novel proteins. By skipping exon 7, an internally deleted protein missing the 57 amino acids encoded by exon 7 will be generated (transcript C in Figure 5). Additional transcripts that initiate at the authentic *Axin* promoter (transcripts D–F) will generate a truncated version of the protein containing the first 637 amino acids of Axin protein [based on the use of the AUG codon at base 391 of the cDNA (ZENG *et al.* 1997)] followed by 65 amino acids derived from the translation of IAP sequence before a termination codon is encountered. The 3′ $Axin^{Kb}$ transcript identified in Figure 6A is unlikely to generate a protein containing the carboxy terminus of Axin, as the two potential in-frame AUGs are preceded by two out-of-frame AUG codons, one of which is contained within a close match to the Kozak consensus sequence for optimal translation initiation (GCCATGG) (KOZAK 1986; 1989) and would generate a five-amino acid peptide. Nevertheless there is the potential for the 3′ transcript to generate either a 168- or a 148-amino acid carboxy-terminal Axin protein.

Aside from the wild-type Axin protein, initiation of transcription at the $Axin^{Fu}$ promoter (transcript B in Figure 5) is predicted to generate an amino terminal peptide that is 47 amino acids shorter than the $Axin^{Kb}$ fragment, as the result of a termination codon immediately after the exon 6 junction. As in the case of $Axin^{Kb}$, it is unlikely that the 3′ transcript produces a fragment of Axin protein, as the first potential in-frame AUG is preceded by four out-of-frame AUG codons, one of which has a good Kozak consensus sequence (GTCAG CATGG), and predicts a different five-amino acid peptide than the one predicted in $Axin^{Kb}$.

DISCUSSION

The visible kinky-tailed phenotype of the dominant mutations in *Fu*, now renamed *Axin*, allowed the gene to be identified 60 years ago (REED 1937). The kinked tail was attributed to duplications in the posterior neural tube, resulting in transient fetal tailbud bifurcations and asymmetrical fusions of ribs and vertebrae, leading to kinking and shortening of the tail (GLUECKSOHN-

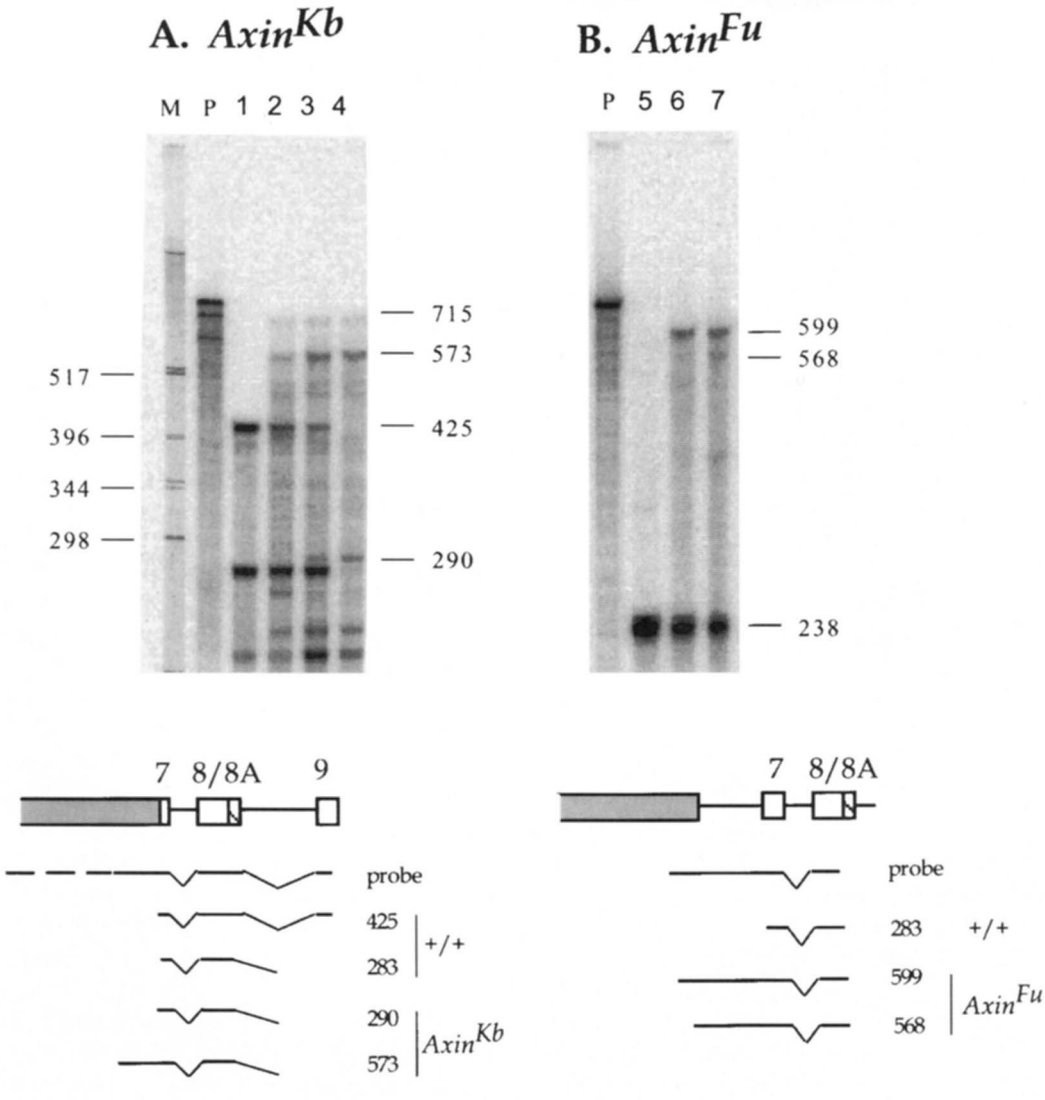

FIGURE 6.—Identification of $Axin^{Fu}$ and $Axin^{Kb}$ transcripts that initiate within the 3′ LTRs. (A) A radiolabeled antisense cDNA probe that spans from 290 bp within the 3′ LTR of $Axin^{Kb}$ to base 2720 in exon 9 was hybridized to wild-type (+/+; lane 2), $Axin^{Kb}$/+ (lane 3) and $Axin^{Kb}/Axin^{Kb}$ (lane 4) RNAs. The protected fragments were analyzed by acrylamide gel electrophoresis. The sizes of the protected fragments are indicated on the right and the sizes of markers on the left (M). P is the probe. (B) A radiolabeled antisense cDNA probe that spans from P2 within the 3′ LTR of $Axin^{Kb}$ to P3 in exon 8 was hybridized to wild-type (+/+; lane 5), $Axin^{Fu}$/+ (lane 6) and $Axin^{Fu}/Axin^{Fu}$ (lane 7) RNAs. The protected fragments were analyzed by acrylamide gel electrophoresis, and the sizes of the protected fragments are indicated on the right. P is the probe. Below each gel the structures and sizes of the probes and protected fragments in A and B are drawn. The regions representing the LTRs are shaded, and the exons are numbered.

SCHOENHEIMER 1949; JACOBS-COHEN *et al.* 1984). Two lines of evidence had supported the proposal that the mutation was a gain-of-function: the absence of kinked tails in animals heterozygous for a deletion of a large chromosomal region surrounding *Axin* (GREENSPAN and O'BRIEN 1986) or a transgene insertion into the gene (PERRY *et al.* 1995), and the retention of a kinked tail in $Axin^{Ki}$ animals with two copies of the wild-type gene (RUVINSKY and AGULNIK 1991). The elucidation of the structure of the *Axin* gene in two semi-dominant alleles, $Axin^{Kb}$ and $Axin^{Fu}$, provides a plausible molecular explanation for the gain-of-function model.

Both mutations result from the insertion of an IAP retrotransposon into the gene, within 456 bp of one another. In the case of $Axin^{Fu}$, the insertion does not disrupt the production of wild-type Axin protein, as the insertion occurs within the sixth intron. Thus the viability of $Axin^{Fu}$ homozygotes is readily explained. In the case of $Axin^{Kb}$, the insertion occurs within exon 7, thereby preventing the synthesis of the normal protein product. $Axin^{Kb}$ homozygotes, in fact, are indistinguishable in phenotype from animals homozygous for the recessive transgene insertion allele $Axin^{Tg1}$, which eliminates the production of the 3.9-kb *Axin* RNA (ZENG *et al.* 1997).

A third allele of *Axin*, *Kinky*, was described in 1940 (CASPARI and DAVID 1940; DUNN and GLUECKSOHN-WAELSCH 1954). In the course of this study we discovered that our stock of $Axin^{Ki}$ mice were, in fact, $Axin^{Kb}$ mice, the confusion having arisen some years ago during a transfer of the mice to the United States from France. GREENSPAN and O'BRIEN (1986) conducted an extensive comparison of the survival of the three dominant alleles as homozygotes and concluded that $Axin^{Ki}$ was the most severe allele, with no homozygous progeny recovered, $Axin^{Kb}$ was intermediate in severity with very small numbers of animal surviving to birth (19% of expected) and $Axin^{Fu}$ was fully viable. However in our experience as well as that of others, both the tail kink and embryonic phenotypes of *Axin* are sensitive to genetic background, which was not uniform in that study. Using two probes tightly linked to *Axin*, $Axin^{Ki}$ and *Ax-*

in^{Kb} could not be distinguished in that study. Unfortunately no DNAs have survived from this study, so it is not possible to examine the molecular nature of the *Axin*^{Ki} allele and to confirm that it was distinct from *Axin*^{Kb}.

The very similar tail phenotypes exhibited by *Axin*^{Fu} and *Axin*^{Kb} suggest that they have the same underlying molecular explanation. This proposal is consistent with the very similar positions of the IAP insertions, which imply that either the site is a hot-spot for retrotransposition or the phenotype is manifested with only a subset of potential integration sites. Such site-specific effects have been observed with the clustered sites of transgene insertions and recombination breakpoints in the mouse *limb deformity* (*ld*) gene that result in the same recessive malformation of the limb (VOGT *et al.* 1992).

The integration of IAP elements through retrotransposition into endogenous genes has been associated with the silencing of the host genes as well as with their inappropriate activation through the action of the strong transcriptional elements within the LTRs (for review see KUFF and LUEDERS 1988). For example, IAP insertions within the 5′ region of the mouse *agouti* gene result in ubiquitous overexpression of the wild-type protein that generates the yellow coat color, obesity, diabetes and tumorigenesis associated with dominant mutations at the locus (DUHL *et al.* 1994; MICHAUD *et al.* 1994). In these instances the IAP LTR overrides the normal transcriptional regulation of the gene. In the case of *Axin*^{Kb}, overexpression or ectopic expression of the wild-type Axin protein is ruled out by the fact that the insertion occurs within an exon.

The insertion of an IAP can also result in the production of chimeric proteins containing fusions of IAP- and host gene-derived segments, the most plausible explanation for the kinked tails in *Axin*^{Fu} and *Axin*^{Kb}. Both *Axin* dominant alleles are predicted by RNA analysis to synthesize an amino terminal fragment of Axin containing the RGS domain coded by exon 2, but lacking the homology to disheveled, found in exons 9 and 10. The proteins would differ in the extent of Axin sequence at their carboxy termini, as well as the inclusion in *Axin*^{Kb} of additional IAP-coded amino acids.

An alternative possibility comes from the observation that both alleles generate a 3′ distal transcript that initiates at the bidirectional promoter in the 3′ LTR and transcribes through the 3′ end of the *Axin* gene. ZENG *et al.* (1997) have recently shown that a deletion of the RGS domain in the amino terminal end of the protein creates a dominant negative form of Axin that can act alone to generate a secondary axis in the ventral region of the Xenopus embryo, presumably by interfering with the inhibitory activity of wild-type Axin in the frog embryo. However given the arguments cited above in favor of the mutations at *Axin* acting as gain-of-function mutations, it seems unlikely that the mutant *Axin*^{Kb} and *Axin*^{Fu} proteins act in this manner in the mouse. Furthermore conceptual translation of the potential 3′ transcripts indicates that the translational machinery would encounter multiple out-of-frame AUG codons before an in-frame AUG is reached. Hence although we cannot rule out the possibility that the dominant mutation is caused by the synthesis of a small peptide or a carboxy-terminal fragment of Axin, we view the synthesis of similar amino terminal fragments as a more likely possibility.

It is also worth noting that we cannot rule out the existence of transcripts that initiate within the 5′-most (relative to *Axin*) LTR of the IAP and transcribe through the 3′ end of the gene. Such transcripts would be impossible to distinguish from those that initiate at the *Axin* promoter, but they would be predicted from RNA analysis to splice in the same manner within the IAP. Finally the bidirectional nature of the promoter in the IAP LTRs (CHRISTY and HUANG 1988) leaves open the possibility that the dominant phenotype is generated by antisense (relative to the *Axin* gene) transcription initiated at either the 5′ or 3′ LTRs. The Northern analysis of adult tissues (Figure 3) failed to identify any transcripts that contain *Axin* sequences 5′ to the insertion site but not 3′ of the site, as this alternative would require, and a sense (relative to *Axin* transcription) RNA probe was not protected from RNAse digestion (data not shown). However it is possible that such transcripts are of low abundance, masked by other transcripts, or silenced in adult tissues, as IAP transcription is known to be more widespread early in development than in later stages (POZNANSKI and CALARCO 1991).

Whatever the nature of the neomorphic protein produced by *Axin*^{Kb} and *Axin*^{Fu}, the kinked tails of the mice are consistent with a perturbation in the development of the most posterior somites, leading to vertebral fusions. Analysis of skeletons of both *Axin*^{Fu} homozygotes and *Axin*^{Kb}/+ heterozygotes revealed no defect in the axial skeleton other than in the tail (T. J. VASICEK, unpublished results).

The somites in the tail bud arise from a different set of mesodermal precursors than the rest of the axial skeleton (TAM and TAN 1992), leaving open the possibility that genes could have specific effects in posterior somites. The restriction of the dominant phenotype of *Axin* to the tail is reminiscent of the selective sensitivity of the tail to heterozygous loss-of-function mutations in the *Brachyury* (*T*) gene. The product of this gene is a T-box-containing transcription factor that is required for the development of all trunk mesoderm (HERRMANN *et al.* 1990). Homozygous *T*/*T* embryos die early in development from a failure of posterior development, but in heterozygotes the only structure affected is the tail, which is shortened or kinked. The tail defect has been attributed to a requirement for higher concentrations of T gene function in the posterior notochord (MACMURRAY and SHIN 1988; STOTT *et al.* 1993). A simi-

lar sensitivity of the tail to reduced dosage of a gene product is evident with hypomorphic alleles of *Wnt-3A* (GRECO *et al.* 1996). Whether the limited effect of the neomorphic Axin proteins is the consequence of a restricted domain of expression of the proteins in the tailbud, or differential sensitivity of the tail to the proteins remains to be determined.

The presence of IAP insertions in both $Axin^{Kb}$ and $Axin^{Fu}$ may help to explain a curious property of the mutations: their variable penetrance that is influenced by the parent-of-origin of the mutation. The penetrance of the tail kinks in *Axin* mutant animals is known to be influenced by genetic background, for example varying between 61% and 88% for two large backcrosses with $Axin^{Kb}$ (ROSSI *et al.* 1994; SUTHERLAND *et al.* 1995). In several studies using both $Axin^{Kb}$ and $Axin^{Fu}$ it has been noted that the penetrance of the kinked tail phenotype was lower in offspring from female mutant parents than male parents (REED 1937; DUNN and CASPARI 1945; DUNN and GLUECKSOHN-WAELSCH 1954; THEILER and GLUECKSOHN-WAELSCH 1956; RUVINSKY and AGULNIK 1990; SUTHERLAND *et al.* 1995). This is reminiscent of the parent-of-origin effects on the severity of the phenotype in the *agouti* IAP insertion alleles (DUHL *et al.* 1994; MICHAUD *et al.* 1994). In the case of both dominant IAP insertion alleles *Avy* and *Aiapy,* female mutant mice produce almost exclusively severely affected offspring whereas male *Avy* mice have between 10% and 34% pseudo-agouti progeny (WOLFF 1971, 1978). The severity of the phenotype was correlated with differences in the DNA methylation of the activating IAP LTR, that is, the more methylated the IAP LTR, the lower the expression of the protein and the less severe the phenotype. Furthermore males were more likely to transmit the IAP in a methylated state than females. This parental difference is consistent with observations that IAPs are more methylated during spermatogenesis than oogenesis (SANFORD *et al.* 1987), and that DNA methylation has a negative effect on LTR activity (LAMB *et al.* 1991).

In the case of *Axin,* the parental bias is in the opposite direction to that in *agouti,* that is, males are more likely to have penetrant offspring. The parent-of-origin effect on the penetrance of *Axin* has been used to suggest that the gene is regulated by genomic imprinting (RUVINSKY and AGULNIK 1990), to the extent that *Axin* is listed on the current map of genomic imprinted regions in the mouse genome (BEECHEY and CATTANACH 1996). The recessive behavior of complete deletions (GREENSPAN and O'BRIEN 1986) and insertions in the *Axin* gene (PERRY *et al.* 1995) now rule out this possibility. However the lower penetrance of *Axin* mutations upon female inheritance, coupled with the observation that the penetrance from *Axin* mothers is reduced even further in the C57BL/6J background (RUVINSKY and AGULNIK 1990) is reminiscent of the effects observed with transgene imprinting (HADCHOUEL *et al.* 1987; REIK *et al.* 1987; SAPIENZA *et al.* 1987; ALLEN *et al.* 1990; SASAKI *et al.* 1991; UEDA *et al.* 1992). In these examples, foreign transgenes were more heavily methylated when inherited from mothers than fathers, and this effect was influenced by genetic background. Whether the parent-of-origin effect on penetrance of the kinked tails can be explained by a modifier that affects the levels of DNA methylation remains to be determined.

In conclusion two dominant mutations in the *Axin* gene result from the insertions of IAP retrotransposons at sites just 456 bp apart. The insertions most probably result in the production of similar neomorphic proteins whose expression affects the development of the most posterior somites, either because of the expression of the neomorphic proteins is restricted to the tailbud, or the most posterior somites are the only tissues sensitive to their presence.

The authors are grateful to Drs. KAREN ARTZT, WILLIAM DOVE and MARY LYON for providing mutant mice and DNA samples. This work was supported by a grant to F.C. from the National Institutes of Health (DK-46934) and the Howard Hughes Medical Institute.

LITERATURE CITED

ALLEN, N. D., M. L. NORRIS and M. A. SURANI, 1990 Epigenetic control of transgene expression and imprinting by genotype-specific modifiers. Cell **61:** 853–861.

AUFFRAY, C., and F. ROUGEON, 1980 Purification of mouse immunoglobulin heavy-chain messenger RNAs from total myeloma tumor RNA. Eur. J. Biochem. **107:** 303–314.

BEECHEY, C. V., and B. M. CATTANACH, 1996 Genetic imprinting map. Mouse Gen. **94:** 96–99.

CASPARI, E., and P. R. DAVID, 1940 The inheritance of a tail abnormality in the house mouse. J. Hered. **31:** 427–431.

CHAN, R. K., and C. A. OTTE, 1982 Physiological characterization of Saccharomyces cerevisiae mutants supersensitive to G1 arrest by a factor and alpha factor pheromones. Mol. Cell Biol. **2:** 21–29.

CHOMCZYNSKI, P., and N. SACCHI, 1987 Single-step method of RNA isolation by acid guanidinium thiocyanate-phenol-chloroform extraction. Anal. Biochem. **162:** 156–159.

CHRISTY, R. J., and R. C. HUANG, 1988 Functional analysis of the long terminal repeats of intracisternal A-particle genes: sequences within the U3 region determine both efficiency and direction of promoter activity. Mol. Cell Biol. **8:** 1093–1102.

DEOL, M. S., 1966 The probable mode of gene action in the circling mutants. Genet. Res. **7:** 363–371.

DIETZEL, C., and J. KURJAN, 1987 Pheromonal regulation and sequence of the Saccharomyces cerevisiae SST2 gene: a model for desensitization to pheromone. Mol. Cell. Biol. **7:** 4169–4177.

DOHLMAN, H. G., and J. THORNER, 1997 RGS proteins: filling in the GAPs in heterotrimeric G protein signalling. J. Biol. Chem. **272:** 3871–3874.

DOHLMAN, H. G., D. APANIESK, Y. CHEN, J. SONG and D. NUSSKERN, 1995 Inhibition of G-protein signaling by dominant gain-of-function mutations in Sst2p, a pheromone desensitization factor in Saccharomyces cerevisiae. Mol. Cell. Biol. **15:** 3635–3643.

DUHL, D. M., H. VRIELING, K. A. MILLER, G. L. WOLFF and G. S. BARSH, 1994 Neomorphic agouti mutations in obese yellow mice. Nature Gen. **8:** 59–65.

DUNN, L. C., and E. CASPARI, 1945 A case of neighboring loci with similar effects. Genetics **30:** 543–568.

DUNN, L. C., and S. GLUECKSOHN-WAELSCH, 1954 A genetical study of the mutation "Fused" in the house mouse, with evidence concerning its allelism with a similar mutation "Kink." J. Genetics **52:** 383–391.

FEINBERG, A. P., and B. VOGELSTEIN, 1984 A technique for radiolabeling DNA restriction endonuclease fragments to high specific activity. Anal. Biochem. **137:** 266–267.

GLUECKSOHN-SCHOENHEIMER, S., 1949 The effects of a lethal mutation responsible for duplications and twinning in mouse embryos. J. Exp. Zool. **110:** 47–76.

GRECO, T. L., S. TAKADA, M. M. NEWHOUSE, J. A. MCMAHON and A. P. MCMAHON, 1996 Analysis of the *vestigial tail* mutation demonstrates that *Wnt-3A* gene dosage regulates mouse axial development. Genes Dev. **10:** 313–324.

GREENSPAN, R. J., and M. C. O'BRIEN, 1986 Genetic analysis of mutations at the fused locus in the mouse. Proc. Natl. Acad. Sci. USA **83:** 4413–4417.

HADCHOUEL, M., H. FARZA, D. SIMON, P. TIOLLIAS and C. POURCEL, 1987 Maternal inhibition of hepatitis B surface antigen gene expression in transgenic mice correlates with *de novo* methylation. Nature **329:** 454–456.

HERRMANN, B. G., S. LABEIT, A. POUSTKA, T. R. KING and H. LEHRACH, 1990 Cloning of the *T* gene required in mesoderm formation in the mouse. Nature **343:** 617–622.

JACOBS-COHEN, R. J., M. SPIEGELMAN, J. C. COOKINGHAM and D. BENNETT, 1984 Knobbly, a new dominant mutation in the mouse that affects embryonic ectoderm organization. Genet. Res. **43:** 43–50.

KLINGENSMITH, J., R. NUSSE and N. PERRIMON, 1994 The *Drosophila* segment polarity gene *dishevelled* encodes a novel protein required for response to the *wingless* signal. Genes Dev. **8:** 118–130.

KOELLE, M. R., and H. R. HORVITZ, 1996 *Egl-10* regulates G protein signaling in the *C. elegans* nervous system and shares a conserved domain with many mammalian proteins. Cell **84:** 115–125.

KOZAK, M., 1986 Point mutations define a sequence flanking the AUG initiator codon that modulates translation by eukaryotic ribosomes. Cell **44:** 283–92.

KOZAK, M., 1989 Circumstances and mechanisms of inhibition of translation by secondary structure in eucaryotic mRNAs. Mol. Cell. Biol. **9:** 5134–5142.

KUFF, E. L., and K. K. LUEDERS, 1988 The intracisternal A-particle gene family: structure and functional aspects. Adv. Cancer Res. **51:** 183–276.

LAMB, B. T., L. L. SATYAMOORTHY, D. SOLTER and C. C. HOWE, 1991 CpG methylation of an endogenous retroviral enhancer inhibits trnscription factor binding and activity. Gene Express. **1:** 185–196.

MACMURRAY, A., and H.-S. SHIN, 1988 The antimorphic nature of the *Tc* allele at the mouse *T* locus. Genetics **120:** 545–550.

MICHAUD, E. J., M. J. VAN VUGT, S. J. BULTMAN, H. O. SWEET and M. T. DAVISSON, 1994 Differential expression of a new dominant agouti allele (*Aiapy*) is correlated with methylation state and is influenced by parental lineage. Genes Dev. **8:** 1463–1472.

MIETZ, J. A., Z. GROSSMAN, K. K. LUEDERS and E. L. KUFF, 1987 Nucleotide sequence of a complete mouse intracisternal A-particle genome: relationship to known aspects of particle assembly and function. J. Virol. **61:** 3020–3029.

NOORDERMEER, J., J. KLINGENSMITH, N. PERRIMON and R. NUSSE, 1994 Dishevelled and armadillo act in the wingless signalling pathway in Drosophila. Nature **367:** 80–83.

PERRY, W. L. I., T. J. VASICEK, J. J. LEE, J. M. ROSSI and L. ZENG, 1995 Phenotypic and molecular analysis of a transgenic insertional allele of the mouse *Fused* locus. Genetics **141:** 321–332.

POZNANSKI, A. A., and P. G. CALARCO, 1991 The expression of intracisternal A particle genes in the preimplantation mouse embryo. Dev. Biol. **143:** 271–281.

REED, C. S., 1937 The inheritance and expression of fused, a new mutation in the house mouse. Genetics **22:** 1–13.

REIK, W., A. COLLICK, M. L. NORRIS, S. C. BARTON and M. A. SURANI, 1987 Genomic imprinting determines methylation of parental alleles in transgenic mice. Nature **328:** 248–251.

ROSSI, J. M., H. CHEN and S. M. TILGHMAN, 1994 Genetic map of the *Fused* locus on mouse chromosome 17. Genomics **23:** 178–184.

RUVINSKY, A. O., and A. I. AGULNIK, 1990 Genetic imprinting and the manifestation of the Fused gene in the house mouse. Dev. Genet. **11:** 263–269.

RUVINSKY, A., A. AGULNIK, S. AGULNIK and M. ROGACHOVA, 1991 Functional analysis of mutations of murine chromosome 17 with the use of tertiary trisomy. Genetics **127:** 781–788.

SANFORD, J. P., H. J. CLARK, V. M. CHAPMAN and J. ROSSANT, 1987 Differences in DNA methylation during oogenesis and spermatogenesis and their persistance during early embryogenesis in the mouse. Genes Dev. **1:** 1039–1046.

SAPIENZA, C., A. C. PETERSON, J. ROSSANT and R. BALLING, 1987 Degree of methylation of transgenes is dependent on gamete of origin. Nature **328:** 251–254.

SASAKI, H., T. HAMADA, T. UEDA, R. SEKI, T. HIGASHINAKAGAWA *et al.*, 1991 Inherited type of allelic methylation variations in a mouse chromosome region where an integrated transgene shows methylation imprinting. Development **111:** 573–581.

STOTT, D., A. KISPERT and B. G. HERRMANN, 1993 Rescue of the tail defect of *Brachyury* mice. Genes Dev. **7:** 197–203.

SUTHERLAND, H. F., E. PICK, E. FRANCIS, H. LEHRACH and A.-M. FRISCHAUF, 1995 Mapping around the *Fused* locus on mouse Chromosome 17. Mammal. Gen. **6:** 449–453.

TAM, P. P. L., and S.-S. TAN, 1992 The somitogenic potential of cells in the primitive streak and tail bud of organogenesis stage mouse embryo. Development **115:** 703–715.

THEILER, K., and S. GLUECKSOHN-WAELSCH, 1956 The morphological effects and the development of the Fused mutation in the mouse. Anat. Rec. **125:** 83–104.

THEISEN, H., J. PURCELL, M. BENNETT, D. KANSAGARA, A. SYED *et al.*, 1994 *dishevelled* is required during *wingless* siganling to establish both cell polarity and cell identity. Development **120:** 347–360.

TSANG, S. S., X. YIN, C. GUZZO-ARDURAN, V. S. JONES and A. J. DAVISON, 1992 One-hour downward alkaline capillary transfer for blotting of DNA and RNA. Anal. Biochem. **201:** 134–139.

UEDA, T., K. YAMAZAKI, R. SUZUKI, H. FUJIMOTO, H. SASAKI *et al.*, 1992 Parental methylation patterns of a transgenic locus in adult somatic tissues are imprinted during gametogenesis. Development **116:** 831–839.

VOGT, T. F., L. JACKSON-GRUSBY, A. J. WYNSHAW-BORIS, D. C. CHAN and P. LEDER, 1992 The same genomic region is disrupted in two transgene-induced *limb deformity* alleles. Mammal. Gen. **3:** 431–437.

WOLFF, G. L., 1971 Genetic modification of homeostatic regulation in the mouse. Am. Nat. **105:** 241–252.

WOLFF, G. L., 1978 Influence of maternal phenotype on metabolic differentiation of agouti locus mutants in the mouse. Genetics **88:** 529–539.

ZENG, L., F. FAGOTTO, T. ZHANG, W. HSU, T. J. VASICEK *et al.*, 1997 The mouse *Fused* locus encodes Axin, an inhibitor of the Wnt signaling pathway that regulates embryonic axis formation in mammals and amphibians. Cell **90:** 181–192.

Communicating editor: R. E. GANSCHOW